Electronic Supplementary Material (ESI) for Journal of Materials Chemistry A.

Supporting Information

Visualization of surface reconstruction and dynamic catalytic sites of Ni-Fe catalysts for oxygen evolution reaction by in-situ Raman measurements

Jia-Wei Zhao,[b#] Kaihang Yue,[c#] Zi-Xiao Shi,[b] Shu-Yin Wei,[b] Wei-Qian Liang,[b] Gao-Ren Li[a*]

[a]College of materials Science and Engineering, Sichuan University, Chengdu 610065, China

[b]School of Chemistry, Sun Yat-sen University, Guangzhou 510275, China

[c]CAS Key Laboratory of Materials for Energy Conversion, Shanghai Institute of Ceramics, Chinese Academy of Sciences (SICCAS), 585 Heshuo Road, Shanghai 200050, China

E-mail: ligaoren@scu.edu.cn

[#]Authors contributed equally to this work.

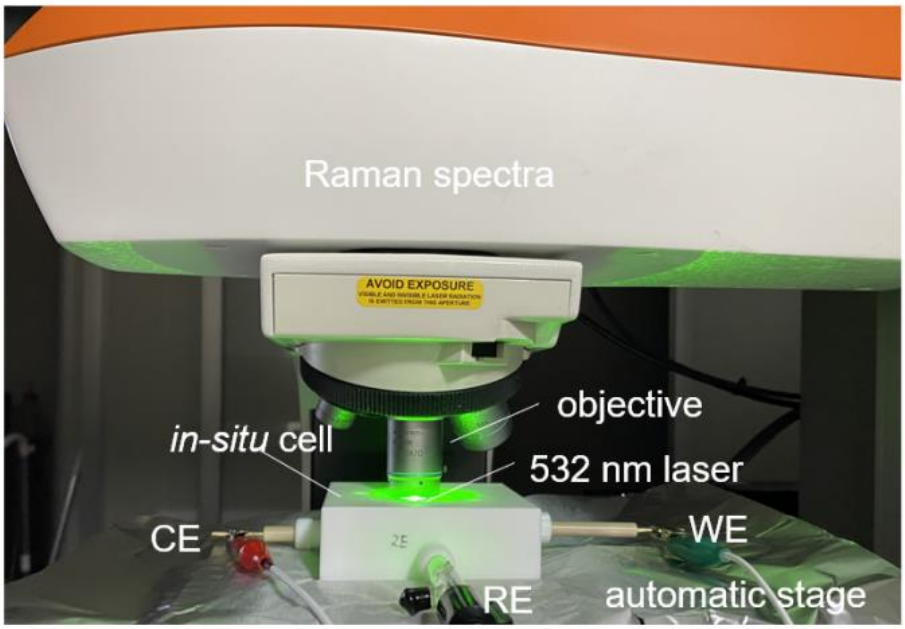

Figure S1. Photograph of In-situ Raman spectra device.

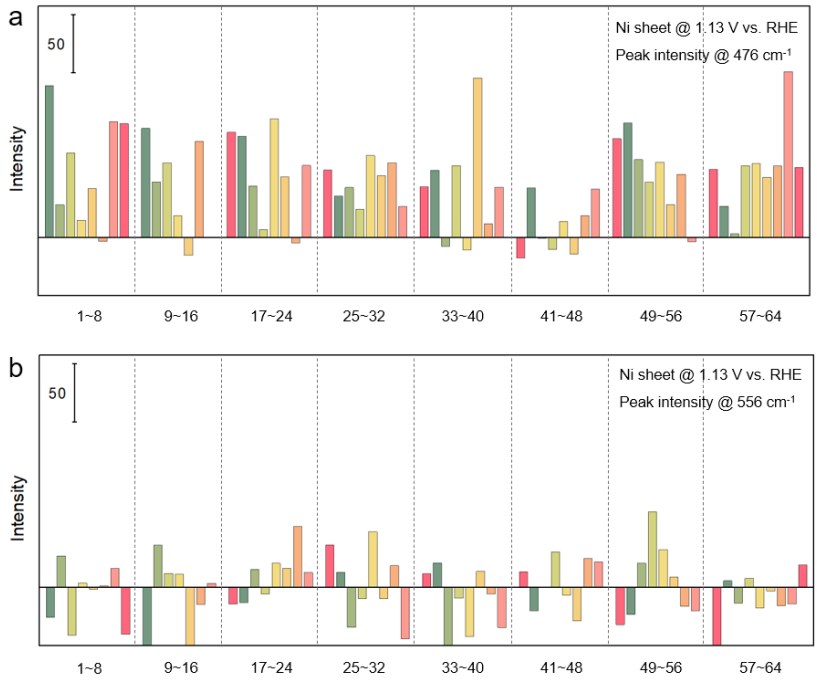

Figure S2. Peak intensities ((a) 476 cm^{-1}, (b) 556 cm^{-1}) of Ni sheet collected by in-situ Raman mapping at 1.13 V vs. RHE.

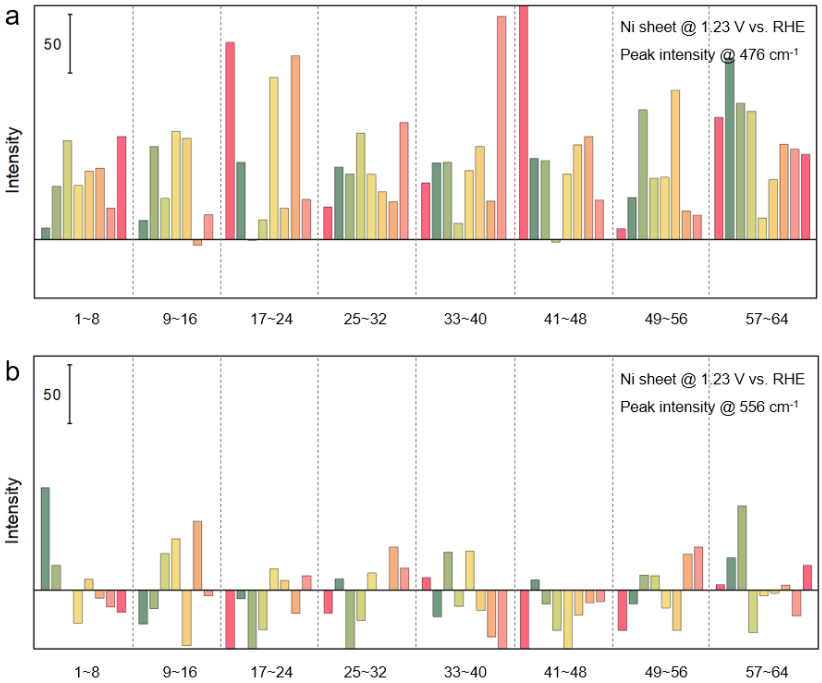

Figure S3. Peak intensities ((a)476 cm^{-1}, (b)556 cm^{-1}) of Ni sheet collected by in-situ Raman mapping at 1.23 V vs. RHE.

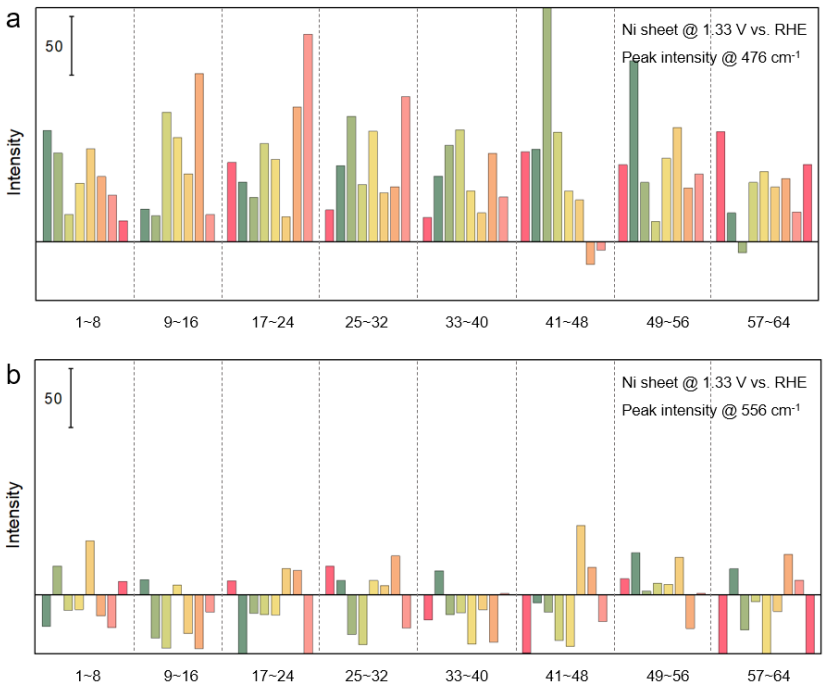

Figure S4. Peak intensities ((a)476 cm^{-1}, (b)556 cm^{-1}) of Ni sheet collected by in-situ Raman mapping at 1.33 V vs. RHE.

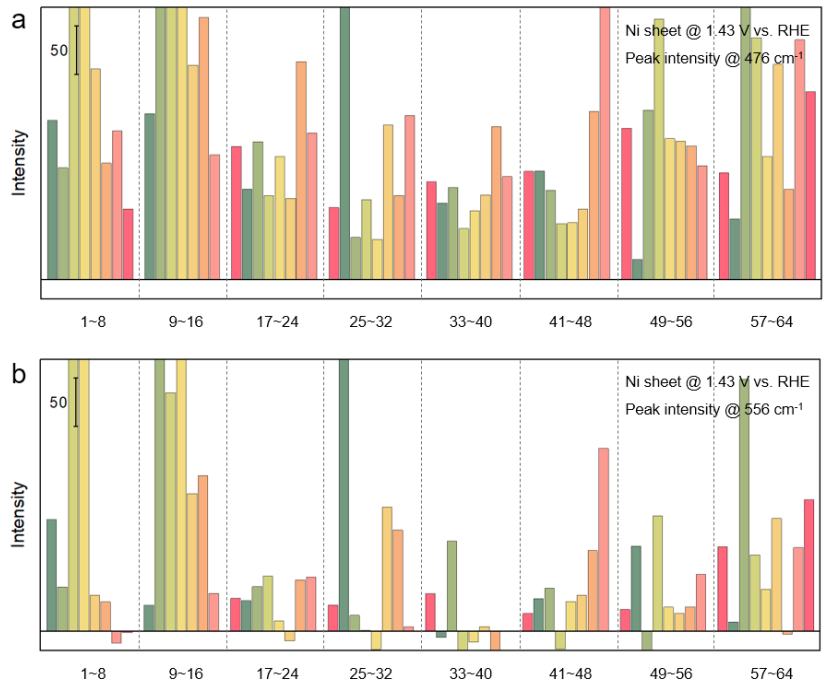

Figure S5. Peak intensities ((a)476 cm^{-1}, (b)556 cm^{-1}) of Ni sheet collected by in-situ Raman mapping at 1.43 V vs. RHE.

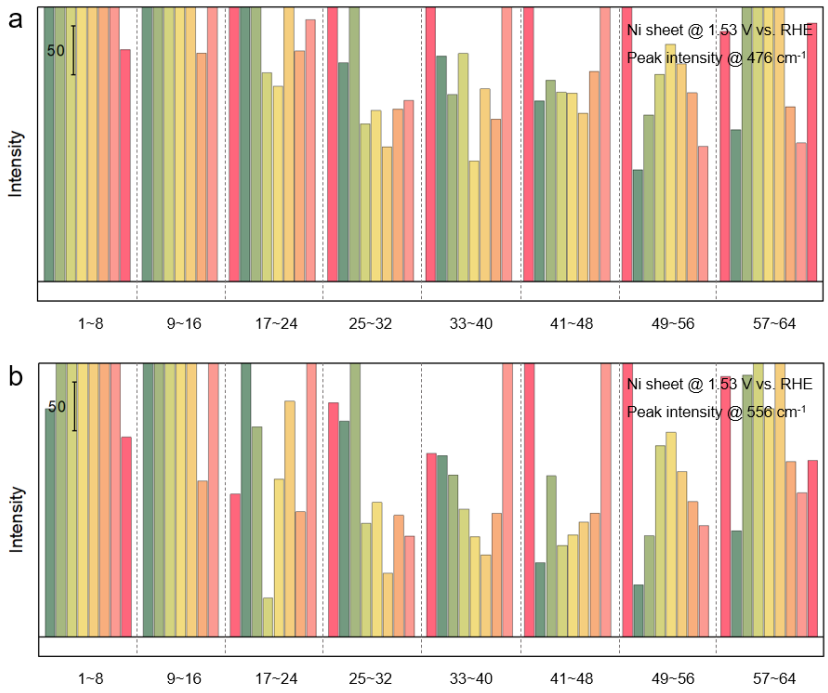

Figure S6. Peak intensities ((a)476 cm^{-1}, (b)556 cm^{-1}) of Ni sheet collected by in-situ Raman mapping at 1.53 V vs. RHE.

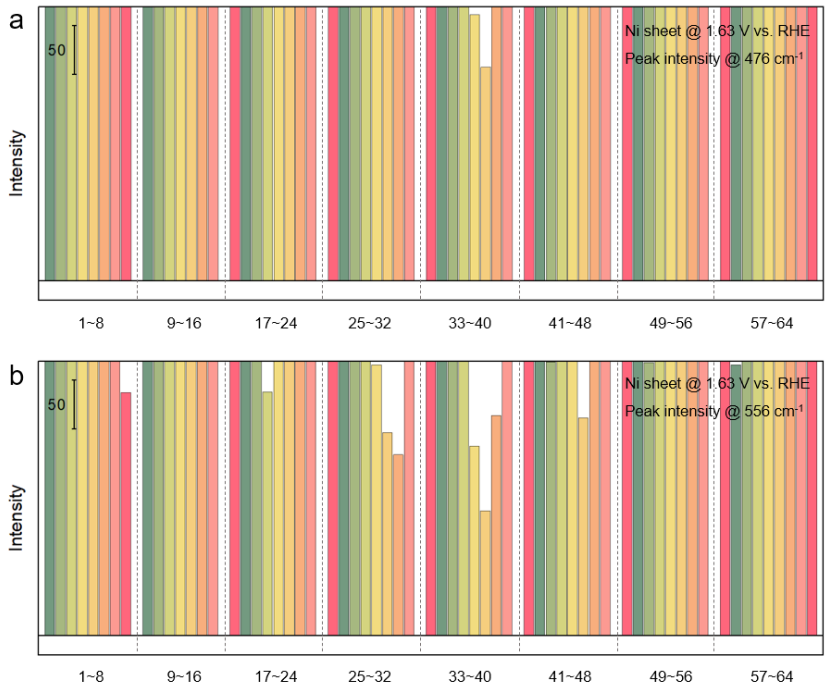

Figure S7. Peak intensities ((a)476 cm^{-1}, (b)556 cm^{-1}) of Ni sheet collected by in-situ Raman mapping at 1.63 V vs. RHE.

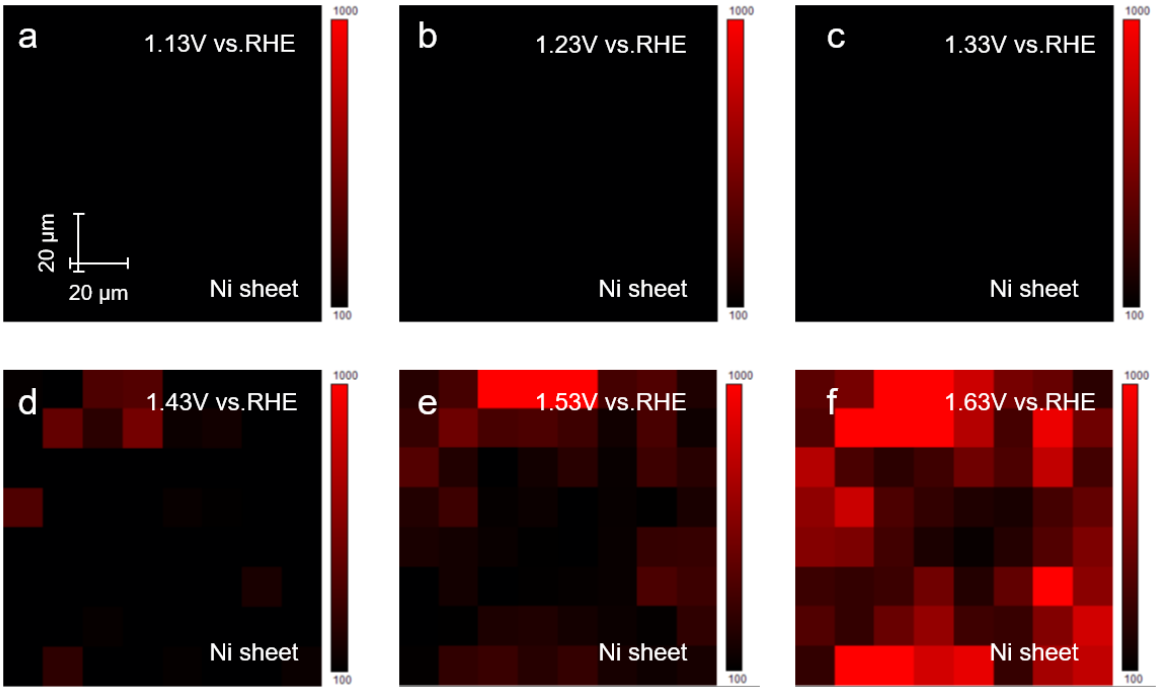

Figure S8. In-situ Raman mappings (peak intensity of 556 cm^{-1}) of Ni sheet at different potentials.

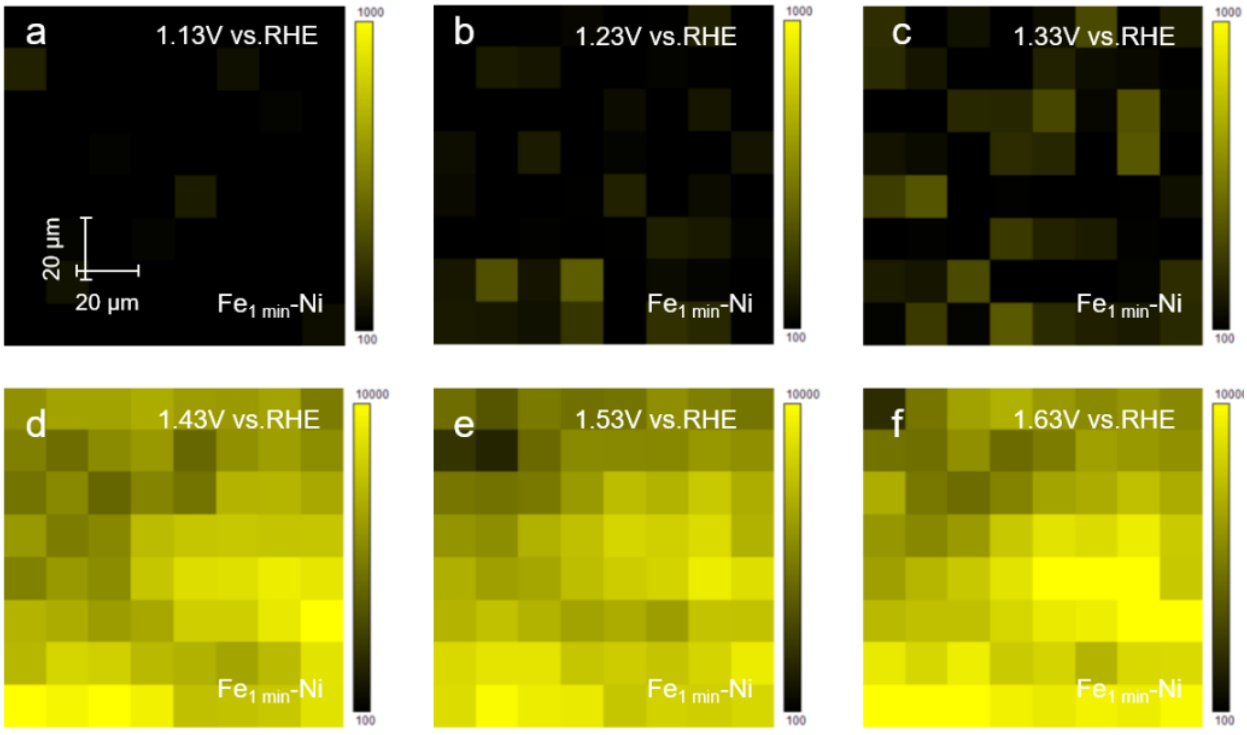

Figure S9. In-situ Raman mappings (peak intensity of 476 cm^{-1}) of Fe_{1min}-Ni sheet at different potentials.

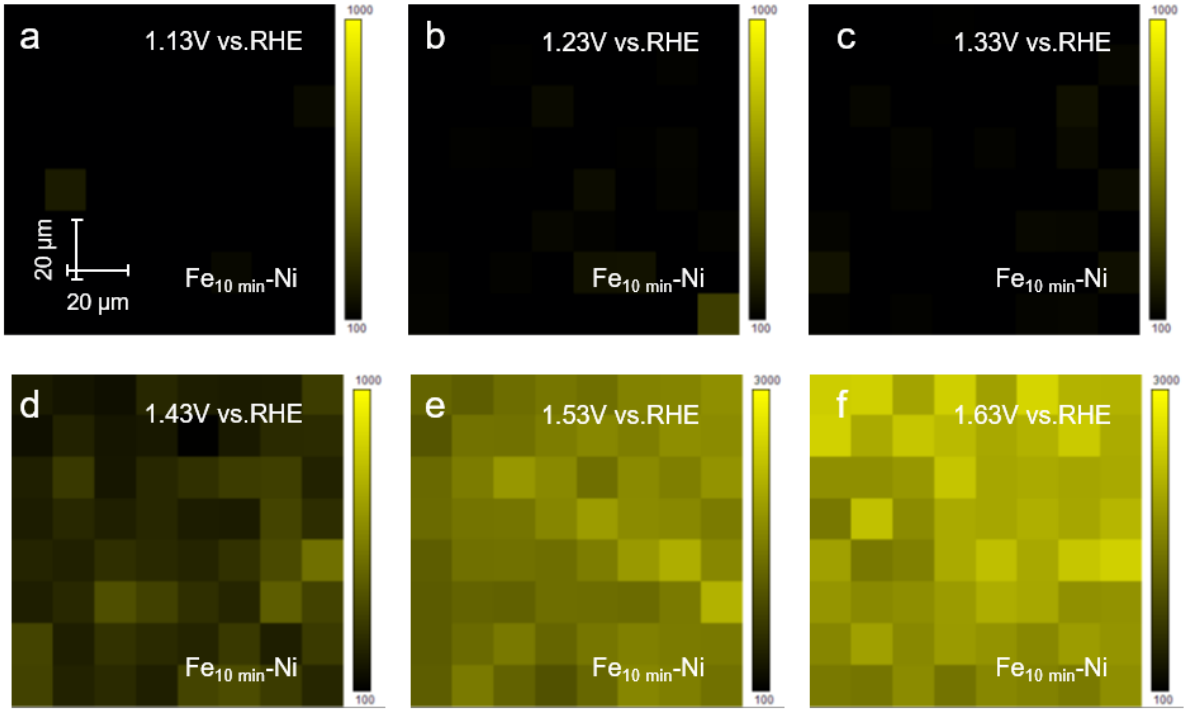

Figure S10. In-situ Raman mappings (peak intensity of 476 cm^{-1}) of Fe_{10min}-Ni sheet at different potentials.

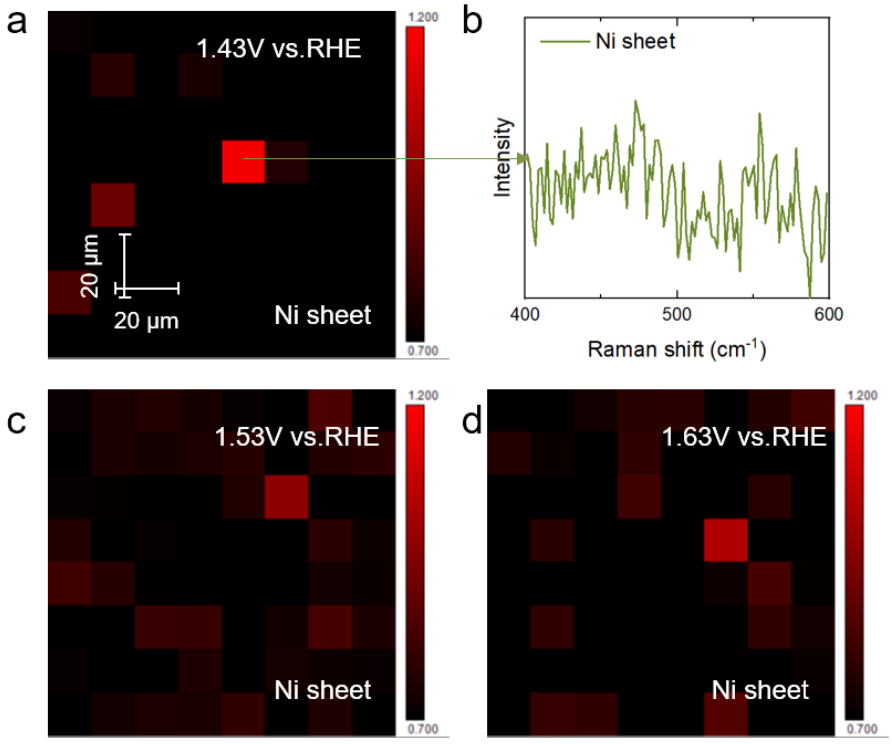

Figure S11. (a, c-d) In-situ Raman mappings (peak ratio of 556 cm^{-1} vs. 476 cm^{-1}) of Ni sheet at different potentials. (b) Special signal of Raman spectrum. This is because the intensity of the two peaks is too weak to accurately determine the ratio of intensity.

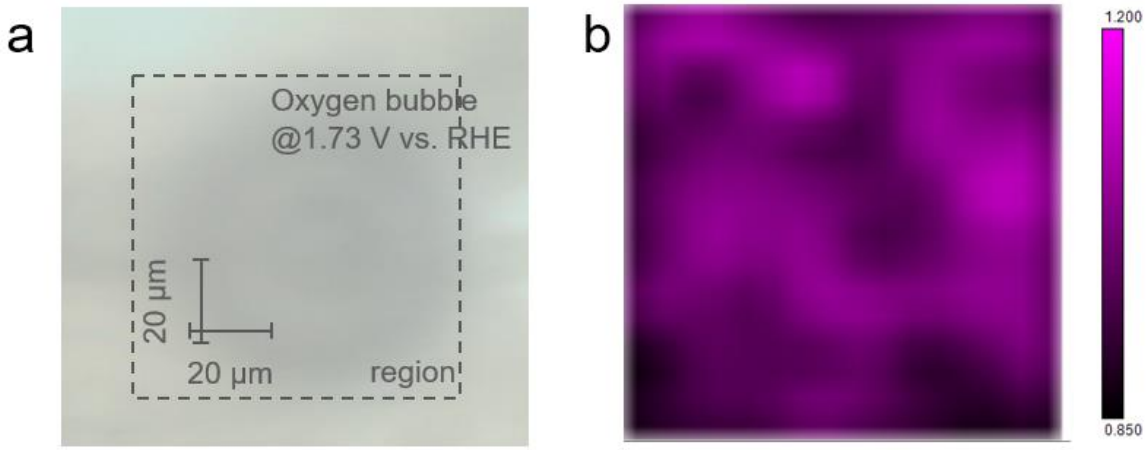

Figure S12. Fe_{10min}-Ni sheet catalytic sites visualized by in-situ Raman mapping.

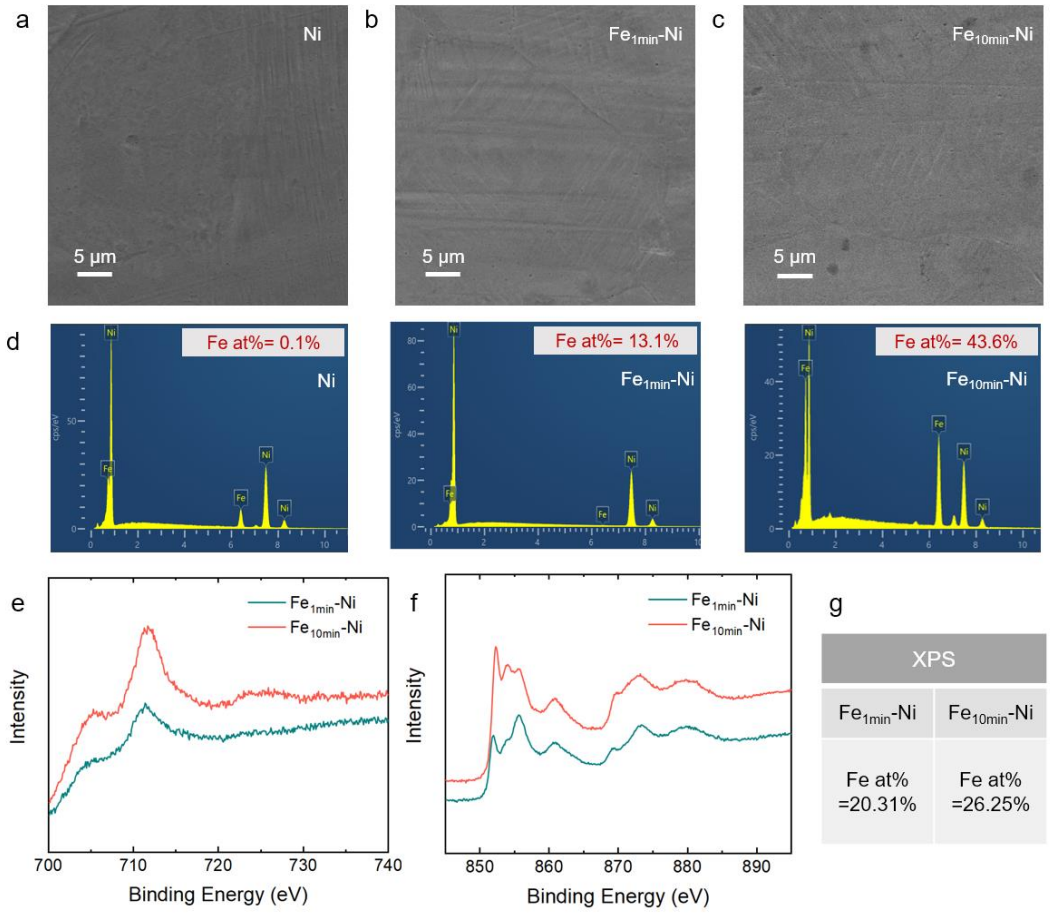

Figure S13. (a-c) SEM images of Ni sheets, Fe_{1min}-Ni and Fe_{10min}-Ni. (d) EDS spectrum of Ni sheets, Fe_{1min}-Ni and Fe_{10min}-Ni. (e) Fe 2p XPS spectra of Fe_{1min}-Ni and Fe_{10min}-Ni. (f) Ni 2p XPS spectra of Fe_{1min}-Ni and Fe_{10min}-Ni. (g) Fe at% of Fe_{1min}-Ni and Fe_{10min}-Ni.

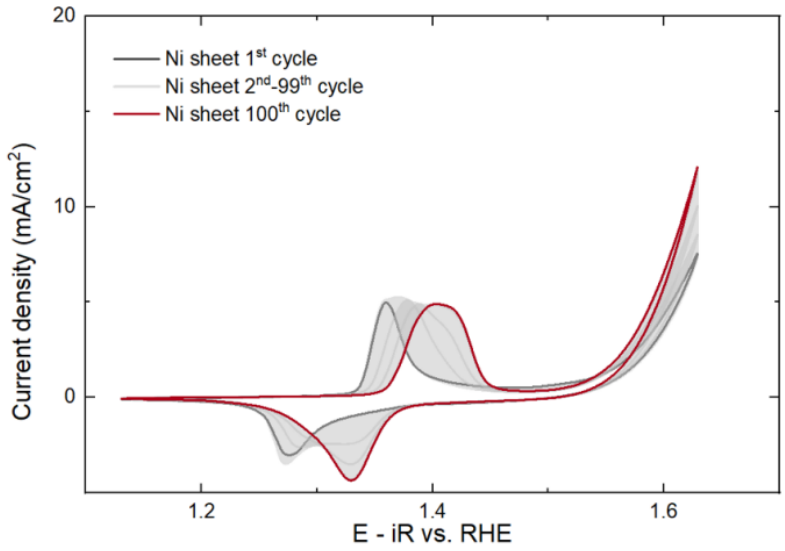

Figure S14. CV curves (1-100 cycles) of Ni sheet.

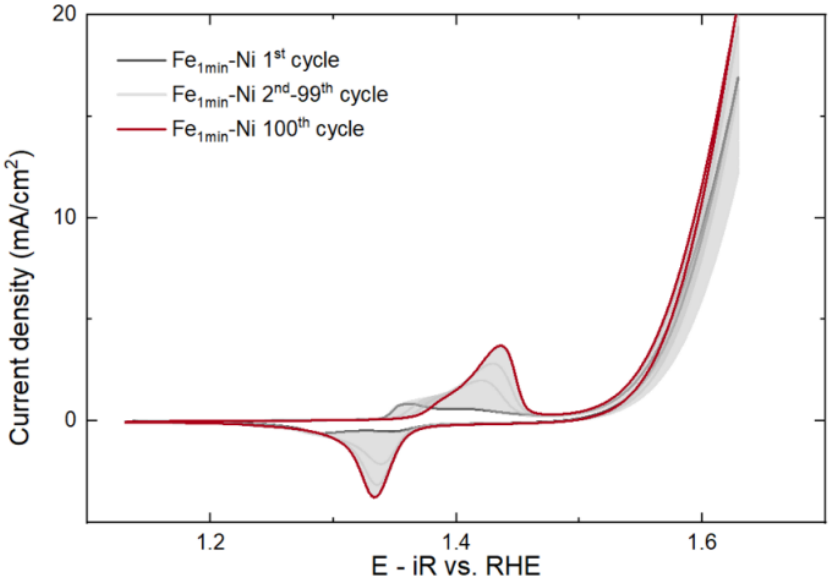

Figure S15. CV curves (1-100 cycles) of Fe_{1min}-Ni sheet.

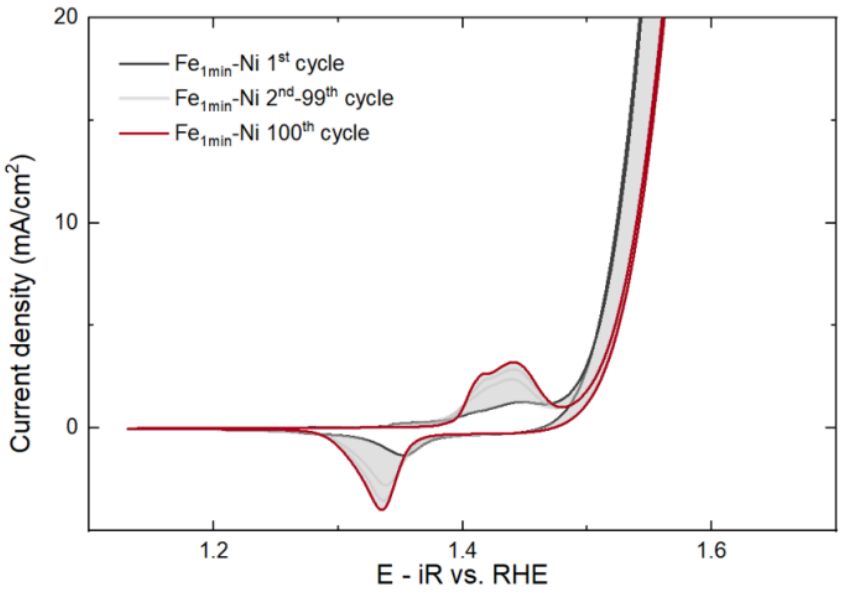

Figure S16. CV curves (1-100 cycles) of Fe_{10min}-Ni sheet.

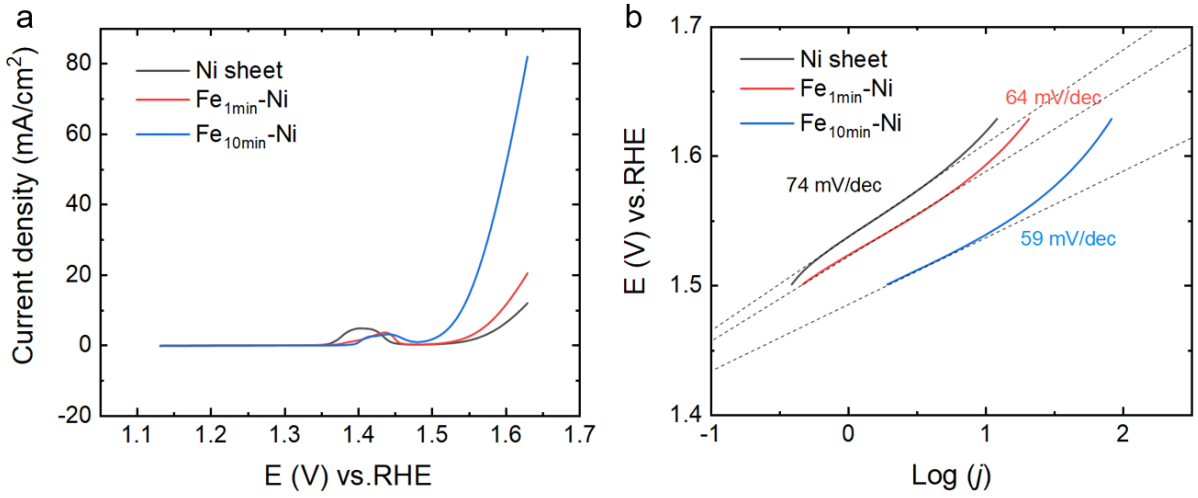

Figure S17. (a) OER performance of Ni sheets, Fe_{1min}-Ni and Fe_{10min}-Ni samples. (b) Tafel plots of Ni sheets, Fe_{1min}-Ni and Fe_{10min}-Ni samples.